Wavelength-selective thermal extraction for higher efficiency and power density thermophotovoltaics

Zoila Jurado, Junlong Kou, Seyedeh Mahsa Kamali, Andrei Faraon, and Austin J. Minnich

Citation: Journal of Applied Physics **124**, 183105 (2018); doi: 10.1063/1.5049733
View online: https://doi.org/10.1063/1.5049733
View Table of Contents: http://aip.scitation.org/toc/jap/124/18
Published by the American Institute of Physics

Wavelength-selective thermal extraction for higher efficiency and power density thermophotovoltaics

Zoila Jurado,[a] Junlong Kou,[a] Seyedeh Mahsa Kamali, Andrei Faraon, and Austin J. Minnich[b]
Division of Engineering and Applied Science, California Institute of Technology, Pasadena, California 91125, USA

(Received 25 July 2018; accepted 24 October 2018; published online 13 November 2018)

Thermophotovoltaics have long been of interest as an energy conversion technology but suffer from low power density and low efficiency. Structured emitters designed to alter the emission spectrum and increase the efficiency are not stable at the necessary high emitter temperatures and also reduce the power density. Here, we propose a wavelength-selective thermal extraction device that mitigates these challenges and demonstrate a transfer-printing process needed to fabricate the device. The device consists of a ZnS solid hemisphere with a patterned thin film optical filter that passively increases the far-field radiated flux from an emitter within a wavelength band near the bandgap of a photovoltaic cell. Crucially, the device does not need to be in physical contact with the emitter and thus can be maintained at a lower temperature, circumventing the thermal stability challenge. Our work helps one to address long-standing issues with applications of thermophotovoltaics. *Published by AIP Publishing.* https://doi.org/10.1063/1.5049733

I. INTRODUCTION

Thermophotovoltaics (TPV) convert heat in the form of electromagnetic radiation directly to electrical energy using a photovoltaic cell (PV),[1] and they have long been of interest due to the possibility to recover energy from waste heat sources as well as their potential to break the Shockley-Queisser limit.[2–4] The majority of losses in a photovoltaic cell (PV) are due to the lack of absorption or thermalization.[5] TPV could reduce these losses provided the emitter spectrum can be altered to emit within a narrow band near the bandgap energy of a PV cell.[5–11]

Numerous works have thus focused on schemes to realize selective emission of the emitted radiation or selective absorption of the incoming radiation combined with photon recycling. For instance, spectral filtering by the PV cell itself has recently been identified as a promising approach to realize >50% efficient TPV systems, but it requires high back-reflector reflectivity and external quantum efficiency of the PV cell.[12] The luminescent bands of rare earth oxides have been proposed for selective emission.[10] However, the spectral emittance and efficiency of these emitters are sensitive to temperature, and the materials may lack the necessary thermal stability. Additionally, rare earth oxides may have a narrow bandwidth resulting in a small overall power density.[9,13,14]

Other efforts have focused on using patterned emitters such as photonic crystals. Metallic photonic crystals have been reported with a modified spectral emissivity compared to unstructured metals.[7,15–17] Refractory metallic ceramics patterned into two-dimensional and three-dimensional inverse opal structures have demonstrated selective thermal emission along with the moderate thermal stability up to 1126 K.[8,11] Unfortunately, the structures degraded after several hours at temperatures exceeding 1300 K. Other methods use external filters such as Bragg stacks to reflect low energy photons, but this filtering reduces the power density.[18] The use of the Bragg stacks as an interference filter between the blackbody emitter and PV cell to tailor emission also leads to peaks in the emission spectrum outside the desired bandpass region.[19] Chase and Joseph[20] and Moller *et al.*[21] first proposed using a cross-mesh array in thin metallic films as a bandpass filter for the infrared region and found that the wavelength peak reflection is determined by the dimensions of the cross. Further contributions by Morgan *et al.* reported the design and fabrication of nanoscale cross-patterned optical filters.[22]

The decreased power density caused by the narrowing of the emission wavelength spectrum for many of the schemes described above impedes applications.[6,23] In principle, this limitation can be overcome by increasing the area of the emitter. Although structured emitters have been realized on a wafer-scale,[24] generally large emitter areas exacerbate fabrication and stability challenges. Utilizing PV cells with smaller bandgaps can in principle increase the maximum power density, but the efficiency of these cells decreases precipitously as the bandgap decreases.[25] This trade-off is a fundamental challenge for the TPV technology.

Therefore, numerous practical challenges complicate the application of TPV. It is clear that a device that increases power density, enables spectral filtering of radiation, and does not suffer from thermal stability challenges would play an important role in furthering TPV. Recent studies suggest that such a device is possible.[26–28] These works reported a passive thermal extraction device consisting of a transparent hemisphere placed in optical contact, but not physical contact, with the emitter. This device enables an enhancement in radiated flux by up to a factor of n^2, where n is the refractive

[a]Z. Jurado and J. Kou contributed equally to this work.
[b]Author to whom correspondence should be addressed: aminnich@caltech.edu

index of the emitter.[29–32] However, the device was not capable of spectrally filtering the emitted radiation and thus thermalization losses and losses due to the lack of absorption would still occur in a TPV system despite the increased power density.

Here, we propose a passive selective thermal extraction device that addresses the power density, spectral filtering, and thermal stability challenges of TPV, and we further demonstrate a transfer-printing process needed to fabricate the device. The passive device consists of an infrared-transparent hemisphere with a patterned thin metal film optical filter that transmits light only around a selected wavelength; other wavelengths are reflected back to the emitter for re-absorption and re-emission. Within the transmitted wavelength band, the radiated flux can be enhanced by up to n^2, where n is the refractive index of the emitting medium. The device can be maintained at a lower temperature than the emitter using a thermal reservoir as the device need only be in optical contact with the emitter. We show that the transfer-printing process preserves key features of the optical transmission spectrum of the filter. Future work will focus on fabricating the entire device and testing its ability to enhance the efficiency of TPV.

II. METHODS

The unpatterned thermal extraction device is a ZnS hemisphere from Crystran Ltd., UK. ZnS transmits radiation between 0.37 and 13.5 μm and possesses a refractive index of 2.36 in the infrared wavelengths.[33] The spectral filter consists of a thin Au film of 50 nm thickness etched with cross patterns that are placed over the hemisphere. The crosses have geometrical dimensions depicted in Fig. 1, designed such that photons at the bandgap energy of InGaAsSb, 0.55 eV (2.25 μm), transmit through the filter.[7] The symmetry of the cross pattern allows for both polarizations of light to be filtered.

The optical filter is fabricated in two steps. The first step is illustrated in Figs. 2(a)–2(c). First, a 300 nm sacrificial layer of Ge is deposited on a 500 μm thick doped Si wafer.[34] Next, electron-beam lithography is used to create a positive, elevated pattern in photoresist ZEP520A. Subsequently, 3 nm of Ti, serving as an adhesion layer, and 50 nm of Au are deposited on the wafer using physical vapor deposition. The second step, Figs. 2(d)–2(f), focuses on the preservation and isolation of the pattern Au layer to obtain the desired optical filter. Prior to lift-off, a layer of a self-assembled monolayer (SAM) is vapor-deposited on the wafer to promote the adhesion of Au.[35] This process is performed by suspending the wafer, as in Fig. 2(c), over 200 μl of (3-mercaptopropyl)trimethoxysilane (MPTMS) in low vacuum (3.1 kPa) for >2 h. Using Remover PG, the electron-beam resist can be removed, leaving the pattern in the optical filter.

The next step is to remove the filter from the Si substrate using transfer printing.[34] Polydimethylsiloxane (PDMS) is spin-coated on a fabricated optical filter at 2000 rpm for 60 s and baked at 80 °C for 1 h. This ~70 μm PDMS layer adds structural stability without compromising the flexibility of the optical filter. The 0.36 cm^2 sample is then immersed in a wet solution of NH_3OH, H_2O_2, and deionized water (2:10:5) for approximately one week. The solution etches the sacrificial layer of Ge, allowing the Au/PDMS film to detach from the substrate and resulting in a robust and flexible optical filter. Finally, the sample can be placed onto a desired substrate. In this work, we demonstrate the transfer printing process by transferring the filter to various substrates and characterize the optical properties of the filter using Fourier-transform infrared spectroscopy (FTIR). All FTIR measurements were taken using a continuum microscope (Spectra-tech Inc. Infinity Reflachromat) to measure specular reflection on a flat surface. In future work, we will measure the spectral transmittance of the filter on a hemisphere and test the device's ability to simultaneously spectrally filter and increase the radiated flux.

III. RESULTS

An SEM image of the final fabricated optical filter on Si is given in Fig. 3(a). The image shows the cross pattern with well-defined edges and good periodicity. Figure 3(b) shows an SEM image of the filter after transfer printing onto another flat substrate. The filter remains mostly intact; the inset image shows that the cross voids generally remain as in the original pattern although with some alteration.

We next proceed to examine the optical properties of the filter before and after transfer printing. First, the reflectance of the filter was calculated using COMSOL with a unit cell of the selective thermal extraction device depicted in Fig. 1. Spectral reflection versus wavelength, shown in Fig. 4(a), shows a minimum reflection around 2 μm, intended to correspond to the bandgap of an InGaAsSb PV cell.[36] The simulated results show that the designed pattern has ~98.5%

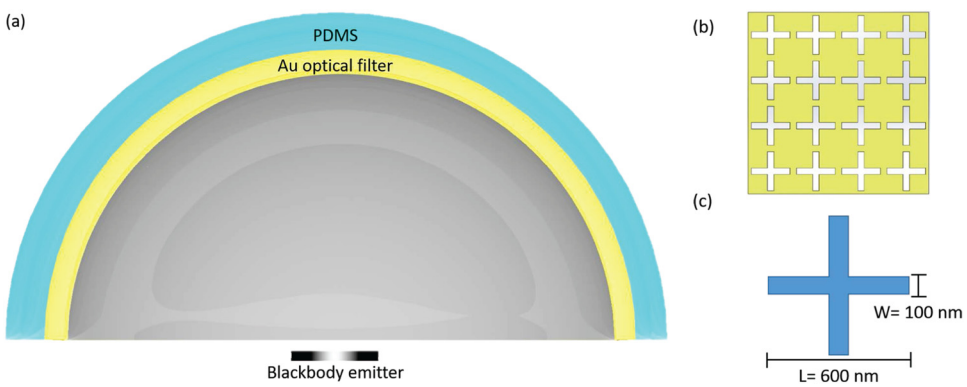

FIG. 1. Schematic cross section of the selective thermal extraction device consisting of a solid ZnS hemisphere covered with an Au optical filter with a cross-void pattern. The PDMS layer is used for the transfer printing process. A PV cell would surround the device in a TPV system. (b) Schematic of cross pattern used to spectrally filter the outgoing radiation. (c) Geometrical parameters of the cross pattern; leg width (W) of 100 nm and total length (L) of 600 nm.

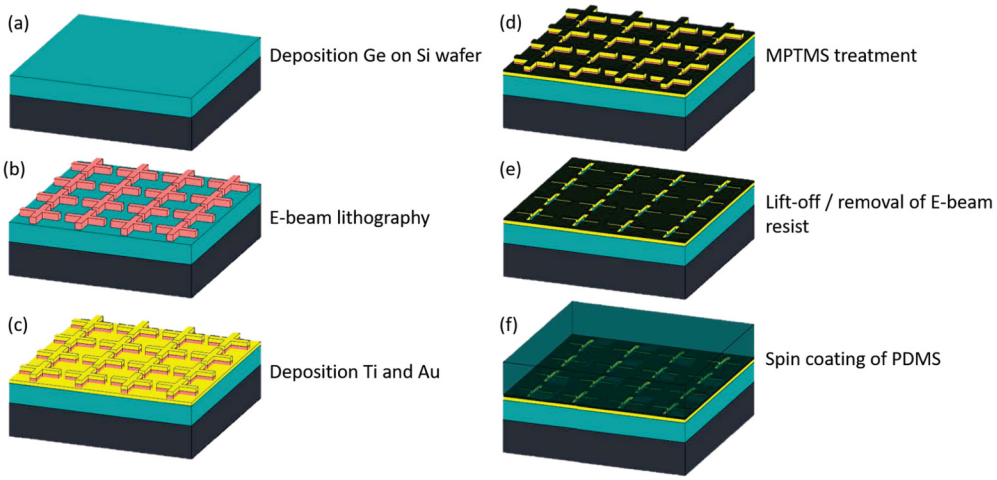

FIG. 2. Schematic illustration of the fabrication process of the optical filter. (a) Deposition of a 300 nm sacrificial layer of Ge on a Si wafer. (b) Spin-coating of positive electron beam resist and patterning using electron beam lithography. (c) Deposition of a 3 nm of Ti adhesion layer and a 50 nm layer of Au. (d) Vapor-deposited MPTMS [(3-mercaptopropyl)trimethoxysilane] surface modification to promote adhesion between Au and PDMS layers. (e) Lift-off to create the Au optical filter and removal of any remaining resist. (f) Spin-coating of a PDMS layer to stabilize the Au pattern prior to the removal of the Au optical filter from the fabrication substrate. After this step (not shown), transfer printing is used to transfer the Au/PDMS film to another substrate.

reflection outside the bandpass region and ~1.5% loss due to absorption and transmission. Within the transmission band, the design reflects ~0.02% of the emitted radiation. We can also calculate the transmission of a unit cell of the selective thermal extraction device. The transmission versus wavelength, illustrated in the inset of Fig. 4(a), validates that the filter does transmit light in the low reflectance region. Within the transmission band, the designed pattern has ~90.6% transmission. Based on the simulated results, we can also determine that ~10% of the emitted radiation is expected to be absorbed by the filter between 1.7 and 3.0 μm and ~2.5% outside this band.

We then measured the spectral reflection of the optical filter before transfer printing using FTIR, as shown in Fig. 4(b). The qualitative shape of the measured reflectance of the filter on ZnS is in reasonable agreement with the simulated results with a minimum reflection occurring at ~1.8 μm. The red shift between the actual and simulated spectra is due to differences in the design and actual cross dimensions. The FTIR measurement of spectral reflectance was normalized to that of a solid Au mirror that was used as the background measurement.

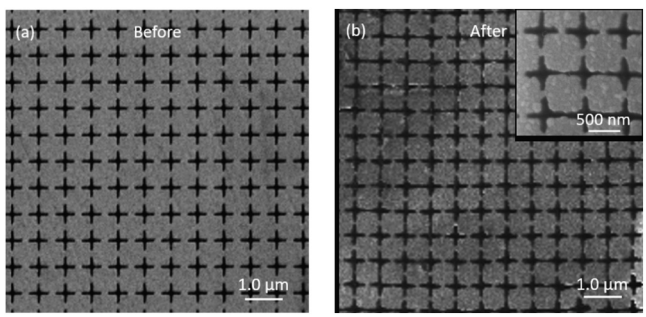

FIG. 3. SEM images of the Au optical filter, before (a) and after (b) the transfer printing process. Inset: zoomed image of the transfer printed filter. The primary features of the pattern are maintained through the transfer printing process.

Next, we suspended the transfer printed optical filter by placing it over a microscope stage with an aperture and measured reflectivity versus wavelength. The wavelength at which the minimum reflection occurs remains nearly the same. The overall selectivity of the transfer printed filter appears to be reduced as indicated by the decrease in reflection outside the pass band. However, the actual overall reflectance is likely larger than measured here as the FTIR only measures the specular reflection; scattered light is not measured. In the actual device, the scattered light would still be returned to the emitter for absorption and re-emission.

The filter can be transfer printed to a spherical surface due to mechanical properties that are similar to those of polyethylene films. The filter coats the 5 mm diameter ZnS hemisphere conformally although with wrinkles that are expected when a planar surface is placed on a spherical object. Due to experimental challenges associated with measuring optical properties of the curved surface, we were unable to obtain optical spectra of this device; this effort will be the subject of future work.

IV. DISCUSSION

We now examine the capability of the device to address the challenges of TPV. First, we note that the thermal extraction device will increase the power density of a TPV system by a factor of n^2. Using the ZnS hemisphere with $n = 2.36$, the device would yield around a factor of 5.6 increase in power density compared to that without thermal extraction.

Second, thermal stability is no longer a requirement because the device is in optical contact, not in physical contact, with the emitter. As the filter does absorb some fraction of the radiation, we perform a simple estimation of the expected temperature rise of the device using the known thermal conductivity of ZnS and the heat input. The filter's average absorption over the blackbody spectrum is 3.48%, and so the total absorbed radiation from an emitter at 1500 K is 55.6 kWm^{-2}. Therefore, for a hemisphere with a radius of

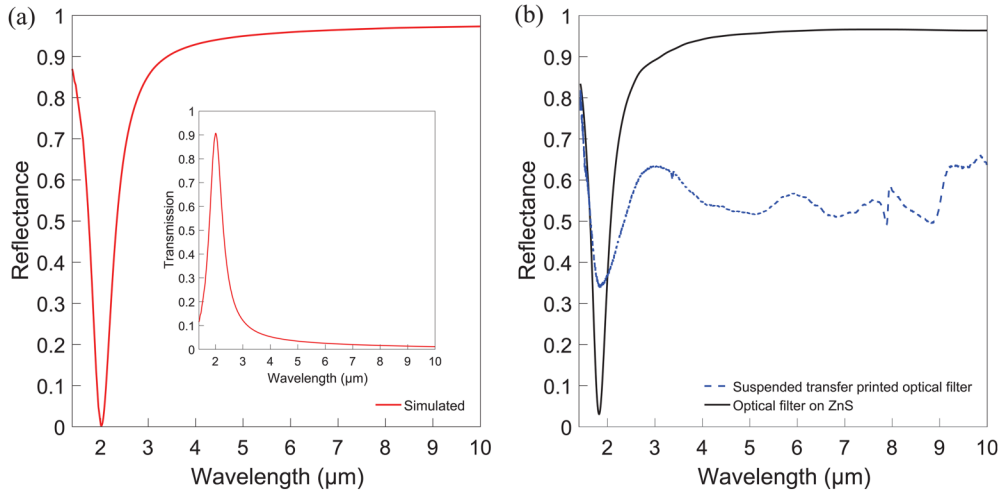

FIG. 4. The (a) simulated and (b) experimental reflectance versus wavelength of the Au filter depicted in Fig. 1. Inset: simulated transmission versus wavelength. The unit cell is composed of the 50 nm Au cross-void pattern and an approximately 70 μm thick PDMS layer. The measured reflectance of the filter prior to lift-off (black) is in reasonable agreement with the simulated results. The measured reflectance of the filter after transfer printing (blue) maintains a minimum at a wavelength of 2 μm. The reflectance for wavelengths outside the bandpass is decreased, which may be due to diffuse reflection of the light that is not measured in the FTIR.

2.5 mm, the device will absorb ~2.2 W. The edges of the flat surface of the hemisphere are assumed to be maintained at a given temperature. Using a thermal resistor model at steady state, we estimate the temperature difference between the filter and the bottom edge of the device. Taking the distance between hot and cold as $L \approx r$ and an approximate cross-sectional area as $A_c \approx \pi r^2$, we estimate the peak temperature rise on the order of 1 K, demonstrating that the device can be maintained at a different, lower temperature than the emitter using a thermal reservoir.

Finally, we use the simulated optical reflectivity and transmission curves to determine the ideal increase in the efficiency and power density. Figure 5 illustrates the distribution of spectral irradiance of a blackbody at $T = 1500$ K to the far-field between 0 and 10 μm. Without the spectral filter, the total irradiance is 1.60 MWm^{-2}, including the n^2 factor due to the hemisphere. In the presence of the optical filter, we calculate that 72.2% of the emitted flux will be reflected back to the emitter to be re-absorbed, meaning 1.15 MWm^{-2} will be recovered. From the reflectance curves in Fig. 4(a), it is also seen that 24.4% of the reflected light has energy exceeding that of the TPV cell bandgap.

We use these values to calculate the increase in the efficiency of a TPV device that incorporates the filter. We assume that the solar cell has a hemispherical shape surrounding the thermal extraction device. Using the Shockley-Queisser analysis[2] and following the notation from Ref. 35, the solar cell efficiency (η_{sc}) is given by[2,37]

$$\eta_{sc} = U(T, E_g)v(T, E_g)m(V_{op}). \quad (1)$$

The first term in Eq. (1) is the ultimate efficiency of a photoelectric device with a single bandgap. It assumes that all photons with $E \geq E_g$ produce one electron-hole pair with voltage of $V_g = E_g/q$. In our calculations, we take the transmitted photons to be equivalent to the emitted photons. Therefore, the emitted photons with the spectral filter are equal to the transmission curve, Fig. 4(a) inset, multiplied by the blackbody distribution at 1500 K. The second term in Eq. (1) originates from the inequality of the open-circuit voltage and the bandgap voltage. We assume an ideal solar cell with a hemispherical geometry for both the emitter and the cell such that the non-ideality factor is equal to that of an ideal solar cell system with planar geometry. Finally, the third term in Eq. (1) is the impedance matching factor.

Using Eq. (1), we calculated the efficiency under three conditions: (1) $T = 6000$ K, $E_g = 1.1$ eV without the spectral filter; (2) $T = 1500$ K, $E_g = 0.55$ eV without the spectral filter, and (3) $T = 1500$ K, $E_g = 0.55$ eV with the spectral filter. The theoretical efficiencies are 40.6%, 24.4%, and 51.2%, respectively. Therefore, the ideal spectral filter will increase the maximum efficiency from 24.4% to 51.2% while simultaneously increasing the power density by ~5 as mentioned previously.

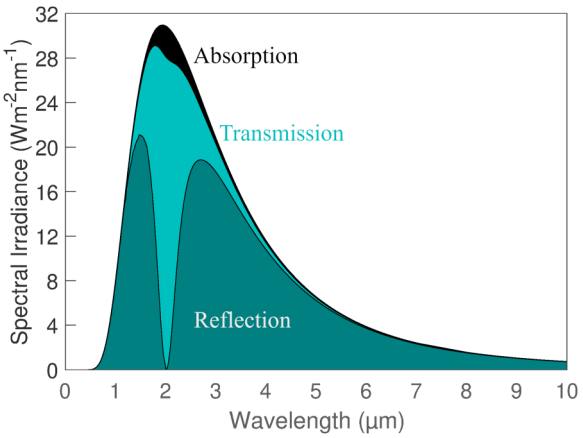

FIG. 5. The calculated distribution of the filtered spectral irradiance of a blackbody at $T = 1500$ K to the far-field between 0 and 10 μm, based on the simulated reflection and transmission curves shown in Fig. 4(a). The total absorbed, transmitted, and reflected energy are indicated by black, turquoise, and teal, respectively.

V. SUMMARY

In summary, we propose a selective thermal extraction device that addresses several of the key challenges of TPV and demonstrates a transfer printing process that is necessary to fabricate the device. The device has the potential to achieve simultaneous spectral filtering and enhancement of radiative flux beyond the apparent blackbody limit of the emitter using thermal extraction. The thermal stability challenge is eliminated as the device need not be in physical contact with the emitter. Our work helps one to address challenges associated with the application of the TPV technology.

ACKNOWLEDGMENTS

This work is part of the "Light-Material Interactions in Energy Conversion" Energy Frontier Research Center funded by the U.S. Department of Energy, Office of Science, Office of Basic Energy Sciences under Award No. DE-SC0001293. The authors would also like to recognize the Kavli NanoScience Institute at Caltech and Professor George R. Rossman and Dr. Alireza Ghaffari of Caltech for the use of their facilities for fabrication and testing.

[1]B. D. Wedlock, "Thermo-photo-voltaic energy conversion," Proc. IEEE **51**, 694–698 (1963).
[2]W. Shockley and H. J. Queisser, "Detailed balance limit of efficiency of p-n junction solar cells," J. Appl. Phys. **32**, 510–519 (1961).
[3]T. Coutts and J. Ward, "Thermophotovoltaic and photovoltaic conversion at high-flux densities," IEEE Trans. Electron Devices **46**, 2145–2153 (1999).
[4]N.-P. Harder and P. Wurfel, "Theoretical limits of thermophotovoltaic solar energy conversion," Semicond. Sci. Technol. **18**, S151–S157 (2003).
[5]A. Polman and H. A. Atwater, "Photonic design principles for ultrahigh-efficiency photovoltaics," Nat. Mater. **11**, 174–177 (2012).
[6]D. M. Bierman, A. Lenert, W. R. Chan, B. Bhatia, I. Celanovic, M. Soljacic, and E. N. Wang, "Enhanced photovoltaic energy conversion using thermally based spectral shaping," Nat. Energy **1**, 16068 (2016).
[7]X. Liu, T. Tyler, T. Starr, A. R. Starr, N. M. Jokerst, and W. J. Padilla, "Taming the blackbody with infrared metamaterials as selective thermal emitters," Phys. Rev. Lett. **107**, 045901 (2011).
[8]K. A. Arpin, M. D. Losego, A. N. Cloud, H. Ning, J. Mallek, N. P. Sergeant, L. Zhu, Z. Yu, B. Kalanyan, G. N. Parsons, G. S. Girolami, J. R. Abelson, S. Fan, and P. V. Braun, "Three-dimensional self-assembled photonic crystals with high temperature stability for thermal emission modification," Nat. Commun. **4**, 2630 (2013).
[9]D. L. Chubb, A. T. Pal, M. O. Patton, and P. P. Jenkins, "Rare earth doped high temperature ceramic selective emitters," J. Eur. Ceram. Soc. **19**, 2551–2562 (1999).
[10]G. Torsello, M. Lamascolo, A. Licciulli, D. Diso, S. Tundo, and M. Mazzer, "The origin of highly efficient selective emission in rare-earth oxides for thermophotovoltaic applications," Nat. Mater. **3**, 632–637 (2004).
[11]S. Y. Lin, J. Moreno, and J. G. Fleming, "Three-dimensional photonic-crystal emitter for thermal photovoltaic power generation," Appl. Phys. Lett. **83**, 380 (2003).
[12]V. Ganapati, T. P. Xiao, and E. Yablonovitch, "Ultra-efficient thermophotovoltaics exploiting spectral filtering by the photovoltaic band-edge," e-print https://arxiv.org/abs/1611.03544 (2018).
[13]A. Licciuli, D. Diso, G. Torsello, S. Tundo, A. Maffezzoli, M. Lomascolo, and M. Mazzer, "The challenge of high performance selective emitters for thermophotovoltaic applications," Semicond. Sci. Technol. **18**, S174–S183 (2003).
[14]A. Boccolini, J. Marques-Hueso, D. Chen, Y. Wang, and B. S. Richards, "Physical performance limitations of luminescent down-conversion layers for photovoltaic applications," Solar Energy Mater. Solar Energy **122**, 8–14 (2014).
[15]S. Y. Lin, J. G. Fleming, D. L. Hetherington, B. K. Smith, R. Biswas, K. M. Ho, M. M. Sigalas, W. Zubrzycki, S. R. Kurtz, and J. Bur, "A three-dimensional photonic crystal operating at infrared wavelengths," Nature **394**, 251–253 (1998).
[16]V. Rinnerbauer, Y. X. Yeng, W. R. Chan, J. J. Senkevich, J. D. Joannopoulos, M. Soljacic, and I. Celanovic, "High-temperature stability and selective thermal emission of polycrystalline tantalum photonic crystals," Opt. Express **21**, 11482–11491 (2013).
[17]V. Rinnerbauer, A. Lenert, D. M. Bierman, Y. X. Yeng, W. R. Chan, R. D. Geil, J. J. Senkevich, J. D. Joannopoulos, E. N. Wang, M. Soljacic, and I. Celanovic, "Metallic photonic crystal absorber-emitter for efficient spectral control in high-temperature solar thermophotovoltaics," Adv. Energy Mater. **4**, 1400334 (2014).
[18]O. Ilic, P. Bermel, G. Chen, J. D. Joannopoulos, I. Celanovic, and M. Soljacic, "Tailoring high-temperature radiation and the resurrection of the incandescent source," Nat. Nanotechnol. **11**, 320–324 (2016).
[19]A. Leroy, B. Bhatia, K. Wilke, O. Ilic, M. Soljacic, and E. N. Wang, "Combined selective emitter and filter for high performance incandescent lighting," Appl. Phys. Lett. **111**, 094103 (2017).
[20]S. T. Chase and R. D. Joseph, "Resonant array bandpass filters for the far infrared," Appl. Opt. **22**, 1775–1779 (1983).
[21]K. D. Moller, J. B. Warren, J. B. Heaney, and C. Kotecki, "Cross-shaped bandpass filter for the near- and mid-infrared wavelength regions," Appl. Opt. **35**, 6210–6215 (1996).
[22]M. D. Morgan, W. E. Horne, V. Sundaram, J. C. Wolfe, S. V. Pendharkar, and R. Tiberio, "Application of optical filters fabricated by masked ion beam lithography," J. Vac. Sci. Technol. B **14**, 3903–3906 (1996).
[23]P. F. Baldasaro, J. E. Raynolds, G. W. Charache, D. M. DePoy, C. T. Ballinger, T. Donovan, and J. M. Borrego, "Thermodynamic analysis of thermophotovoltaic efficiency and power density tradeoffs," J. Appl. Phys. **89**, 3319–3327 (2001).
[24]V. Rinnerbauer, S. Ndao, Y. X. Yeng, J. J. Senkevich, K. F. Jensen, J. D. Joannopoulos, M. Soljacic, I. Celanovic, and R. D. Geil, "Large-area fabrication of high aspect ratio tantalum photonic crystals for high temperature selective emitters," J. Vac. Sci. Technol. B **31**, 011802 (2013).
[25]W. R. Chana, P. Bermel, R. C. N. Pilawa-Podgurskie, C. H. Marton, K. F. Jensen, J. J. Senkevich, J. D. Joannopoulos, M. Soljacic, and I. Celanovic, "Toward high-energy-density, high-efficiency, and moderate-temperature chip-scale thermophotovoltaics," Proc. Natl. Acad. Sci. USA **110**, 5309–5314 (2013).
[26]Z. Yu, N. P. Sergeant, T. Skauli, G. Zhang, H. Wang, and S. Fan, "Enhancing far-field thermal emission with thermal extraction," Nat. Commun. **4**, 1730 (2013).
[27]C. Lin, B. Wang, K. H. Teo, and Z. Zhang, "Near-field enhancement of thermoradiative devices," J. Appl. Phys. **122**, 143102 (2017).
[28]Y. Yang and L. Wang, "Spectrally enhancing near-field radiative transfer between metallic gratings by exciting magnetic polaritons in nanometric vacuum gaps," Phys. Rev. Lett. **117**, 044301 (2016).
[29]E. Yablonovitch, "Statistical ray optics," Opt. Soc. Am. **72**, 899–907 (1982).
[30]J. L. Pan, H. K. H. Choy, J. Clifton, and G. Fonstad, "Very large radiative transfer over small distances from a black body for thermophotovoltaic applications," IEEE Trans. Electron Devices **47**, 241–249 (2000).
[31]A. Narayanaswamy and G. Chen, "Surface modes for near field thermophotovoltaics," Appl. Phys. Lett. **82**, 3544 (2003).
[32]E. G. Cravalho, C. L. Tien, and R. P. Caren, "Effect of small spacings on radiative transfer between two dielectrics," J. Heat Transf. Trans. ASME **89**, 351–358 (1967).
[33]Crystran, "Zinc sulphide multispectral," see https://www.crystran.co.uk/optical-materials/zinc-sulphide-multispectr al-zinc-sulfide-zns.
[34]S. M. Kamali, A. Arbabi, E. Arbabi, Y. Horie, and A. Faraon, "Decoupling optical function and geometrical form using conformal flexible dielectric metasurfaces," Nat. Commun. **7**, 11618 (2016).
[35]I. Byun, A. W. Coleman, and B. Kim, "Transfer of thin Au films to polydimethylsiloxane (PDMS) with reliable bonding using (3-mercaptopropyl)trimethoxysilane (MPTMS) as a molecular adhesive," J. Micromech. Microeng. **23**, 085016 (2013).
[36]G. W. Charache, P. F. Baldasaro, L. R. Danielson, D. M. DePoy, M. J. Freeman, C. A. Wang, H. K. Choi, D. Z. Garbuzov, R. U. Martinelli, V. Khalfin, S. Saroop, J. M. Borrego, and R. J.Gutmann, "InGaAsSb thermophotovoltaic diode: Physics evaluation," J. Appl. Phys. **85**, 2247–2252 (1999).
[37]E. Rephaeli and S. Fan, "Absorber and emitter for solar thermalphotovoltaics systems to achieve efficiency exceeding the Shockley-Queisser limit," Opt. Express **17**, 15145–15159 (2009).